NIH Public Access
Author Manuscript
Semin Nucl Med. Author manuscript; available in PMC 2014 July 01.

Published in final edited form as:
Semin Nucl Med. 2013 July ; 43(4): 271–280. doi:10.1053/j.semnuclmed.2013.03.003.

Radionuclide Methods and Instrumentation for Breast Cancer Detection and Diagnosis

Suleman Surti, PhD
Department of Radiology, Perelman School of Medicine at the University of Pennsylvania, Philadelphia, PA

Abstract

Breast cancer mammography is a well-acknowledged technique for patient screening due to its high sensitivity. However, in addition to its low specificity the sensitivity of mammography is limited when imaging patients with dense breasts. Radionuclide imaging techniques, such as coincidence photon-based positron emission tomography and single photon emission computed tomography or scintimammography, can play a role in assisting screening of such patients. Radionuclide techniques can also be useful in assessing treatment response of patients with breast cancer to therapy, and staging of patients to diagnose the disease extent. However, the performance of these imaging modalities is generally limited because of the poor spatial resolution and sensitivity of the commercially available multipurpose imaging systems. Here, we describe some of the dedicated imaging systems (positron emission mammography [PEM] and breast-specific gamma imaging [BSGI]) that have been developed both commercially and in research laboratories for radionuclide imaging of breast cancer. Clinical studies with dedicated PEM scanners show improved sensitivity to detecting cancer in patients when using PEM in conjunction with additional imaging modalities, such as magnetic resonance imaging or mammography or both, as well as improved disease staging that can have an effect on surgical planning. High-resolution BSGI systems are more widely available commercially and several clinical studies have shown very high sensitivity and specificity in detecting cancer in high-risk patients. Further development of dedicated PEM and BSGI systems is ongoing, promising further expansion of radionuclide imaging techniques in the realm of breast cancer detection and treatment.

Breast cancer is the most prevalent form of cancer in women, with an incidence rate that is twice that of lung cancer, the next higher form. Several studies have shown that detection and treatment of breast cancer in the early stages lead to a decrease in breast cancer mortality rates.[1–4] As a result, mammographic imaging with an average sensitivity rate of 80%–90% is used as a screening tool for early detection of breast cancer. However, for women with dense breasts (about 40% of women undergoing mammography[5]) the sensitivity range drops to 50%–85%.[6] Another study[7] of a large sample of patients has shown that the specificity of mammography is only 35.8% and results in a large fraction of false-positive cases. These considerations suggest that other modalities such as radionuclide imaging might be helpful in breast cancer diagnosis in clinical scenarios where a mammography's performance is limited. Radionuclide imaging might offer advantages over other modalities used for breast imaging, such as magnetic resonance imaging (MRI) and ultrasound (US), in the conspicuity of tumors, with resulting more facile imaging interpretation.

© 2013 Elsevier Inc. All rights reserved.

Address reprint requests to: Suleman Surti, PhD, Department of Radiology, Perelman School of Medicine at the University of Pennsylvania, 404 Blockley Hall, 423 Guardian Drive, Philadelphia, PA 19104. surti@mail.med.upenn.edu.

NIH-PA Author Manuscript
NIH-PA Author Manuscript
NIH-PA Author Manuscript

NIH-PA Author Manuscript

NIH-PA Author Manuscript

NIH-PA Author Manuscript

Another area of application of radionuclide imaging lies in assessing treatment response of a primary tumor to therapy. Traditional techniques, such as mammography or US, depend on anatomical or morphologic changes in the tumor size to determine the efficacy of ongoing treatment, and require up to 3 cycles of treatment before any conclusions can be made.[8] Radionuclide imaging, by providing functional information can lead to an early assessment of the treatment before any anatomical or morphologic changes are observed in the tumor. An early assessment of treatment response would help in patient management by either continuing with the ongoing therapy for responding patients or using alterative therapy plans for nonresponding patients. A recent study[9] found that primary tumor ^{18}F-Fluorodeoxyglucose (FDG) standardized uptake value obtained by whole-body positron emission tomography (PET) decreased in responders after the first round of chemotherapy (responders determined by pathology results after 6 rounds of therapy). Using 60% of the baseline standardized uptake value as the cutoff, whole-body PET had a sensitivity of 61% and specificity of 96% in determining the responders after just 1 round of chemotherapy.

Finally, radionuclide imaging can also play a role in staging of a patient with breast cancer by determining the extent of disease in the breast. An accurate definition of the extent of disease can help choose between various treatment options, especially with respect to breast conservation or mastectomy. This has also been examined as a role for radionuclide imaging and is discussed elsewhere in this review series.

Early radionuclide imaging studies[10–13] demonstrated high sensitivity for detecting malignant lesions in patients with larger, often palpable lesions, but subsequent experience has shown a limited sensitivity for detection of small lesions.[1–4] In particular, in a large PET study[14] it was found that the clinical detection sensitivity of PET is <48% for all pT1 stage tumors (<2 cm in size) and <9% for tumors <1 cm in size (pT1a and pT1b stages). Currently, the 2 primary radionuclide imaging techniques for breast cancer are PET imaging and single photon planar scintimammography or single photon-based emission computed tomography (SPECT) imaging. Both clinical PET and single photon imaging systems have limited spatial resolution and sensitivity that limits their use in detecting small lesions, as well as accurately measuring the lesion uptake to determine the tumor response to therapy. For example, clinical PET scanners achieve reasonably good spatial resolution in the range of about 5–6 mm[15,16] with large scanner ring diameters of about 90 cm. Breast imaging, however, is concerned with detecting, characterizing the nature, and monitoring the response of small tumors in the early pT1 (lesion size is as small as 5 mm or less (pT1a stage)[14]) and pT2 (lesion size <2 cm) stages, and hence the scanner resolution and sensitivity would be inadequate. For clinical single photon imaging systems, the spatial resolution and sensitivity are worse than in clinical PET that further compromises their application to breast imaging. Hence, there has been a push toward developing radionuclide imaging systems dedicated specifically for breast imaging. They can be broadly labeled as positron emission mammography (PEM, for PET radiopharmaceuticals) and breast-specific gamma imaging systems (BSGI, for SPECT radiopharmaceuticals). In this review, we highlight devices that have been developed for PEM and BSGI, including clinical trials of existing devices, and ongoing work in breast imaging instrumentation designed to further improve performance.

PEM Systems

A dedicated breast PET scanner producing tomographic images with very high spatial resolution and sensitivity relative to all-purpose whole-body PET scanners can play a significant role in the screening and staging of breast cancer in women. In particular, a dedicated breast scanner can provide quantitative tumor response measures owing to the accurate uptake measurements (high spatial resolution) achieved in a dynamic imaging mode (high sensitivity) for early assessment of response to neoadjuvant therapy. A dedicated

NIH-PA Author Manuscript

NIH-PA Author Manuscript

NIH-PA Author Manuscript

breast PET scanner could also serve as a component in a multimodality breast imaging device, in combination with either a mammography or a tomosynthesis unit, optical scanner, US, or even MRI. Biologically, it is known that ^{18}F-FDG may not be the ideal tracer for breast cancer imaging, but new tracers[17] developed to study processes such as cellular proliferation (^{18}F-fluorothymidine) and apoptosis (^{18}F labeled annexin V) in breast cancer, as well as estrogen-receptor imaging for breast cancer (^{18}F-fluoroestradiol), may all benefit with the use of dedicated breast PET scanners. Although research is ongoing in the development of new tracers, in parallel there is a significant effort being put into the development of dedicated PET devices as well.

The cost of a small, high performance dedicated breast scanner can be significantly less than a clinical whole-body PET/computed tomography (PET/CT) because of the use of less detector material (uses about 5% of scintillator volume present in a clinical scanner). Compared with a clinical whole-body PET/CT, the solid angle coverage is also larger (about a factor of 2.5) with 2 detectors placed close to the breast in a dedicated scanner. Using 10-mm long LYSO crystals in the breast scanner, for example, would translate into a point source in air sensitivity similar to that achieved in clinical whole-body scanners (5%–8%),[18–20] which use 20–30-mm long LSO or LYSO crystals. A dedicated breast scanner, however, also has the advantage of reduced attenuation of coincident photons because they do not travel through the chest (factor of 10 increase in sensitivity) before reaching the detector, leading to an equivalent factor of 10 gain in total sensitivity over the clinical scanner. Besides the significant gain in sensitivity over a clinical PET scanner, a dedicated breast scanner can also have a much higher spatial resolution (1–2 mm as opposed to 5–6 mm in a clinical scanner) that would allow detection and quantification of small lesions (5 mm or less in diameter), a task that is practically impossible in reasonable scan times on a clinical scanner. Considering a typical scan time of 3 minutes per single bed position (for imaging 2 breasts) on a clinical scanner, a dedicated breast scanner would, therefore, lead to higher quality images of the breast in similar scan times because of a higher number of collected counts and better spatial resolution. It should also be kept in mind that scans on a clinical PET scanner are normally performed for a whole-body imaging protocol, and so the total scan time on a clinical scanner is much longer (anywhere between 15–45 minutes). As a result, significant technological effort has been exerted over many years, focused towards the development of dedicated PEM devices. Most of this effort has been within academic research groups with only recent entry of commercial vendors.

Stationary Flat Detector-Based PEM Scanners for Imaging Compressed Breast

One of the first dedicated PEM system was the PEM-I device developed at the Montreal Neurological Institute, which used 2 planar Bismuth Germanate detectors coupled to arrays of position-sensitive photomultiplier tubes (PSPMTs).[21,22] Each detector was 20-mm thick leading to high sensitivity, and was pixelated into 1.9-mm wide crystals with a 2-level depth-of-interaction (DOI) measurement. This detector design led to high spatial resolution (2.8 mm) with reduced parallax error in the reconstructed image due to the DOI information. The PEM-I scanner with an imaging field of view (FOV) of 6.5 cm × 5.5 cm was installed on a standard mammography system providing images of the compressed breast using an iterative limited-angle image reconstruction algorithm with the ability to coregister with the mammograms.

Similar flat detector system designs that image compressed breast have subsequently been developed and evaluated by different research groups. One system developed at the National Institutes of Health used 1-cm thick Bismuth Germanate detectors coupled to PSPMTs with a detector FOV of 6.0 cm × 6.0 cm.[23] This system had a spatial resolution of 3.1 mm and was initially incorporated within a mammography gantry as well. An iterative limited-angle image reconstruction algorithm was used to reconstruct the images. Another system with a

NIH-PA Author Manuscript

NIH-PA Author Manuscript

NIH-PA Author Manuscript

larger FOV was developed at the Thomas Jefferson National Laboratory and Duke University using 3 × 3 × 10-mm^3 LGSO crystals coupled to PSPMTs to produce 2 planar detectors with FOV of 15 cm × 20 cm.[24] Spatial resolution of this system was around 4 mm. The detectors were incorporated in a conventional mammography unit and images were reconstructed with an iterative reconstruction algorithm.

Recently, the Naviscan Flex Solo II PEM scanner has become commercially available (Naviscan PET Systems, Inc.) and is the only commercial PEM scanner available for clinical use (Fig. 1). This system uses 2 × 2 × 13-mm^3 LYSO crystals coupled to PSPMTs to form 2 flat detectors with an imaging area of 6 cm × 16.4 cm each. The detectors scan across the imaging FOV along their 6-cm dimension to form an active imaging FOV of 24 cm × 16.4 cm. The Flex Solo II scanner has a dedicated stand-alone upright gantry where the 2 detectors are attached to an articulating arm that rotates for imaging different views as in a conventional mammography scanner. An iterative reconstruction algorithm is used to generate 3D images of the compressed breast. Several clinical studies have been performed in the last few years that utilize the Flex Solo II scanner. In Figure 2 we show an example PEM image[25] of a patient with ductal carcinoma in situ (DCIS) compared with a mammogram, where the PEM image shows intense focal uptake at calcification site.

A recent clinical study[26] evaluated the effect of PEM using Flex Solo II in breast cancer presurgical planning and compared it with MR imaging. This study involved 388 participants (25 years of age or older, median age of 58 years) newly diagnosed with invasive or intraductal breast cancer or both through biopsy (404 index lesions with median tumor size of about 1.5 cm) who were candidates for breast conservation surgery, and who voluntarily underwent PEM and MR imaging within 5 days of each other. For PEM imaging, the patients were injected with an average of 10.9 mCi (403 MBq) of ^{18}F-FDG followed by an average of 69 minutes uptake time before imaging. PEM and MRI images were read independently by the investigators for most cases, but in conjunction with a full knowledge of mammography and prestudy biopsy results. For index lesions, PEM had a sensitivity (specificity) of 92.5% (89%) vs 89.1% (28%) with MRI. Accuracy for detection of index lesions was 89.1% with PEM and 88.4% with MRI. Additional cancer was found in 82 breasts with a total of 305 discrete nonindex lesions identified (median tumor size 0.7 cm). Out of the 305 nonindex lesions, biopsies were performed on 211 and 166 were found to be malignant. The sensitivity, specificity, and accuracy of mammography, MRI, PEM, and MRI + PEM for detecting additional cancer is summarized in Table 1 at the breast and lesion levels. Both MRI and PEM lead to higher sensitivity compared with mammography, whereas a combination of PEM with MRI leads to an additional gain in sensitivity for detecting previously unknown malignant lesions. Although sensitivity of PEM and MRI is similar, with MRI being slightly higher, the specificity of PEM is better compared with MRI.

The study also indicated a potential role for PEM in local breast staging, namely determining the extent of disease in the breast. In this study, 98 patients underwent mastectomy out of which 56 were considered appropriate for the procedure; however, 11 inappropriate procedures were prompted by the imaging findings. Among the 98 patients, the extent of disease estimated accurately, underestimated, and overestimated by PEM (MRI) was 50% (66%), 43% (17%), and 7.1% (16%), respectively. For the 56 patients who required necessary mastectomy, 40 were accurately identified with MRI as opposed to 20 with PEM. Of the 11 patients who underwent unnecessary mastectomy, 10 were overestimated in MRI and 6 in PEM (5 patients overlapped here with overestimation in both MRI and PEM). For breast surgical planning related to the need for mastectomy, MRI had a higher sensitivity but lower specificity compared with PEM in accurately defining the extent of the disease.

NIH-PA Author Manuscript

NIH-PA Author Manuscript

NIH-PA Author Manuscript

Rotating Detector-Based PEM Scanners for Imaging Uncompressed Breast

A different direction chosen by some researchers has been to develop PEM/PET scanners that image a whole breast uncompressed, with the goal being to have an accurate reconstructed image of the breast with full quantitative imaging capability. The Crystal Clear collaboration at CERN has developed the Clear-PEM scanner[27] that uses 2 flat detectors rotating around the imaging FOV to collect data from all projection angles for fully 3D tomographic image reconstruction. Each detector head has dimensions of 16.5 cm × 14.5 cm and is composed of 2 × 2 × 20-mm^3 LYSO crystals coupled directly to an avalanche photodiode array on both ends of the crystal to provide DOI measurement and reduce system parallax error. The patient lies prone on a flat bed with the breast hanging between the 2 rotating detector heads within the imaging FOV. Two other research systems have recently been completed that also utilize 2 rotating PET heads, together with a CT source and a detector, to perform fully integrated dedicated breast PET/CT. In both these systems the patient lies prone on the bed and the breast hangs within the imaging FOV through a small opening. The system at the University of California, Davis is comprised of two, 12-cm × 12-cm flat detector heads that are comprised of 3 × 3 × 20-mm^3 LSO crystals coupled to PSPMTs.[28] The detector separation is variable (allowing for imaging different size breasts in a more optimum configuration), and an iterative reconstruction algorithm is used to achieve tomographic images. Initial pilot studies with 7 patients have shown good imaging performance from this system[29] where the uncompressed breast was imaged for 12.5 minutes to produce quantitative images. The second system developed at the West Virginia University is very similar in design to the University of California, Davis system, except for the PET's detector head.[30] The individual detector heads are 20 cm × 15 cm in size and utilize 2 × 2 × 15-mm^3 LYSO crystals coupled to PSPMTs. An initial pilot study using 5 patients with an imaging time of 3 minutes per breast showed good imaging characteristics.[30]

Stationary Full or Partial Detector Ring-Based PEM Scanners for Imaging Uncompressed Breast

A more conventional PEM system design utilized by some research groups involves a full angular coverage of the FOV using a ring or enclosed box of detectors. A PEM system developed at the Lawrence Berkeley National Laboratory[31] uses two, 10-cm × 7.5-cm and two, 7.5-cm × 7.5-cm flat detector plates to form an enclosed rectangular box with a transverse port of 8.2 cm × 6 cm and an axial length of 5 cm. Each detector plate is comprised of arrays of detector modules, with each module using an 8 × 8-array of 3 × 3 × 30-mm^3 LSO crystals coupled on 1 end to a single PMT and at the other end to an 8 × 8-array of silicon photodiodes. The photodiodes provide the interaction crystal for the photon, whereas the PMT and the photodiode array signal together provide the DOI within the detector module. Another system (MammiPET) uses 12 detector modules to form a 10-sided enclosed polygon with a scanner aperture of 18.6 cm.[32] Each detector uses a 10-mm thick trapezoidal shaped continuous LYSO crystal with an entrance face of 40 mm × 40 mm and an exit face coupled to a PSMT of 50 mm × 50 mm. Owing to the continuous detector design this scanner also provides DOI information. Using a similar concept of continuous detectors, the breast PET (BPET) scanner at the University of Pennsylvania was originally developed using 2 large, curved plate, NaI (Tl) detectors, each having an active area of 28 cm × 21 cm and using 19-mm thick crystals.[33] The 2 detectors were placed on rails with variable detector separation and an iterative algorithm was used to perform limited-angle reconstruction. A small pilot study using volunteer patients demonstrated not only some of the benefits of dedicated breast PET but also the limitations of limited-angle reconstruction.[34] All 3 of these research systems were designed with a horizontal gantry so that the patient lies prone on the bed while the breast hangs within the imaging FOV though a small opening.

NIH-PA Author Manuscript

NIH-PA Author Manuscript

NIH-PA Author Manuscript

Along the lines of the static full ring PET systems, a group in Kyoto University, Japan has developed 2 dedicated breast systems using the same detector modules.[35] Each detector module uses 4 layers of 1.44 × 1.44 × 4.5-mm^3 LGSO crystals (effective detector thickness of 18 mm) coupled to a single 52-mm square position-sensitive photomultiplier tube. The 4 crystal layers can be individually distinguished to provide a 4-level DOI information. The "O" scanner is a full angular coverage system with 12 detector modules forming 1 complete ring and the full scanner is comprised of 3 such rings. The "O" scanner has a ring diameter of 19.5 cm and an axial length of 15.55 cm with the patient lying prone on the table for imaging. The "C" scanner is comprised of 2 partially complete rings of 12 detector modules each with the gap in each ring being equivalent to 2 missing detector modules. The novel design idea behind this geometry was to scan a patient sitting upright (leaning forward) with the detector gap allowing an easy placement of the breast through the chest wall within the imaging FOV. A clinical study published using these 2 scanners[35] evaluated 69 patients who were suspected of having breast cancer based on the results of a physical examination, mammography, US, or MRI. Each patient was injected with ^{18}F-FDG (0.1 mCi/kg (3.7 MBq/kg) of patient weight) and scanned on a clinical whole-body PET/CT after a 60 minutes uptake time for 2–3 minutes/bed position followed by a 5 minutes scan per breast in both the "O" and "C" scanners. The lesion-based sensitivity of the "O" and "C" scanners was 82% and 83%, respectively, as compared with 92% for the clinical PET/CT. The breast-based specificity of the "O" and "C" scanners was 98% and 98%, respectively, as compared with 100% for the clinical PET/CT. As this study recruited patients already suspected of breast cancer based on other imaging studies and a physical examination, the average tumor size was large (26 mm with a range of 4–112 mm). Hence, the performance advantage of the dedicated PET scanners (spatial resolution and sensitivity) may have been negated with respect to the clinical system.

Ongoing PEM System Development

Based on the work done on the development and subsequent evaluation studies performed with the above outlined PEM systems, there are several ongoing projects aiming to further increase the performance and also evaluate new system designs for dedicated breast imaging. A group at Stanford University is actively developing a very high-resolution system using 2 flat detector panels to image compressed breast.[36] Each detector panel will have an imaging area of 10.0 cm × 15.4 cm and will be composed of several stacks of detector modules. Each detector module uses 1 × 1 × 3-mm^3 LSO crystals arranged in 2, 3 (along 3-mm dimension) × 8 arrays innovatively coupled to 2 position-sensitive avalanche photodiodes. The effective crystal thickness for 511 keV photons will be 1.8 cm (4 crystals stacked along the 3-mm dimension). The system is designed to provide 1-mm spatial resolution with a 3-mm DOI resolution in addition to very high system sensitivity for compressed breast imaging. System simulations indicate an ability to distinguish 2.5-mm diameter lesions that would be useful for detecting early stage breast cancer. At the University of Pennsylvania our group is developing a new generation of the BPET scanner using time-of-flight information to assist in image reconstruction of limited-angle data sets.[37] The detector design utilizes 1.5 × 1.5 × 15-mm^3 LYSO crystals coupled to PSPMTs.[38] The system is designed to achieve a 1.5-mm spatial resolution and timing resolution in the range of 300–500 ps that has been shown to assist in achieving good quality tomographic images with a system covering 2/3 of the transverse angular coverage.[37] The system will be designed to image compressed and uncompressed breast without any detector rotation. The University of California, Davis is in the process of upgrading their existing dedicated breast PET/CT[28] with new, high-resolution PET detectors. The new system will be composed of 2 detectors rotating around the breast and will use 1.5 × 1.5 × 20-mm^3 LSO crystals coupled to a position-sensitive avalanche photodiode on 1 side and a PMT on the other side to provide DOI measurement along the crystal thickness (20 mm).[39] At the

NIH-PA Author Manuscript

NIH-PA Author Manuscript

NIH-PA Author Manuscript

Brookhaven National Laboratory a full ring PET system is being developed that will be placed within the breast radiofrequency coil of a 1.5 T MRI scanner to perform simultaneous breast PET/MR imaging. The final system will use 2.2 × 2.2 × 20-mm^3 LYSO crystals coupled to an avalanche photodiode array for signal read out to form a ring of detectors with 14.5-cm diameter and axial length of 9.6 cm.[40,41] A prototype system using shorter crystals and smaller FOV (10.1 cm diameter and 1.8 cm axial length) has been tested on a few patients with encouraging results, showing the technical viability of this system design. Finally, a group at Washington University is using the concept of virtual pinhole PET[42] to develop a high-resolution PET insert that can be placed closed to the breast while the patient is imaged in clinical whole-body PET scanner. By collecting data simultaneously between this insert and the traditional detector ring of the whole-body scanner, it has been shown that one can achieve high spatial resolution and sensitivity needed for breast imaging while utilizing standard clinical PET systems. An added advantage of such a system will be the ability to image the axilla as well as the whole patient that allows diagnosis of the full extent of disease. The insert is designed to be a single flat detector panel (12 cm × 7.5 cm) that comprises 0.8 × 0.8 × 3-mm^3 LSO crystals coupled to silicon photomultiplier arrays and placed close to the patient breast within a Siemens Biograph PET/CT.[43]

BSGI Systems

Although the role of PEM in breast imaging has concentrated not only on screening or detection of breast tumors but also on disease staging, BSGI has focused primarily on detection of tumors, especially in women with dense breasts. Mammography images are defined by the attenuation of x-rays within the breast tissue that varies as a function of breast density. Hence, women with dense breast suffer from low sensitivity (50%–85%)[6] and specificity (35.8%)[7] of mammography. Gamma imaging techniques such as planar scintimammography with ^{99m}Tc can potentially be useful in these situations as the emission image is relatively independent of the breast density. However, poor spatial resolution and sensitivity of clinical devices limits the performance of these systems, with <50% sensitivity in detection of tumors <10 mm in size.[44,45] Hence, dedicated BSGI systems are expected to provide improved performance and clinical use primarily in screening for women with dense breasts.

Commercial Systems

One of the earlier BSGI systems was developed by Dilon Diagnostics and is sold as Dilon 6800. This planar imaging system uses a single 15-cm × 20-cm detector using arrays of 3 × 3 × 6-mm^3 NaI(Tl) detectors coupled to PSPMTs[46] and images the breast with mild compression to provide views similar to mammograms. Imaging is performed with slanted parallel-hole collimators and the system achieves a 6-mm spatial resolution at a distance of 3 cm from the detector head, which is similar to the midplane of a mildly compressed, average-size breast. Another version of this system (Dilon Acella) is also available with a larger detector head (20 cm × 25 cm). Another system available from Digirad uses a single-detector head with a FOV of 40 cm × 31 cm. This system, called Ergo, uses an array of 3 × 3 × 6-mm^3 CsI crystals coupled to silicon photodiodes for signal read out and uses multiple selections of parallel-hole collimators for data acquisition.

A prospective clinical study[47] was performed with the Dilon 6800 system with a goal of evaluating a high-resolution system's performance in detecting occult cancer in high-risk patients. This study enrolled 94 female patients with a high calculated 5-year risk for development of breast cancer. All patients had a normal mammogram with a BI-RADS category of 1 or 2, and underwent a physical exam (also normal) within 6 months of scintmammography. Both the tests were normal. Patients were injected with 25–30 mCi (925–1110 MBq) of ^{99m}Tc sestamibi and scanned 10 minutes later in the craniocaudal (CC)

NIH-PA Author Manuscript

NIH-PA Author Manuscript

NIH-PA Author Manuscript

and mediolateral oblique (MLO) views with a 10 minutes per view per breast. All mammograms and scintimammograms were reviewed and classified by 2 experienced radiologists. Mammograms were also classified for breast density using the BI-RADS breast density category range of 1–5. The scintimammograms were classified with a score ranging from 1 (normal with no focal or diffuse uptake) to 5 (marked focal uptake), and were interpreted without knowledge of patient characteristics and mammography reports. In Figure 3 we show an image of a patient with increased focal uptake as seen in the scintimammogram. Out of 94 patients, 78 had a normal scintimammogram (score of 1–3) who were subsequently classified as normal in a 1-year follow-up clinical examination, mammogram, and scintimammogram. The remaining 16 patients with an abnormal scintimammogram (scores of 4 and 5) underwent a directed US, out of which 11 underwent biopsy owing to focal hypoechoic finding in the US. Out of these 11 patients, 2 were found to have an invasive carcinoma. The 5 patients who did not show any focal hypoechoic finding in the US had normal scintimammograms in the 6-months and 1-year follow-ups. The 2 patients with true-positive findings had a history of breast carcinoma, mammographic BI-RADS breast density category of 2 and 3, and both cancers measured 9 mm in the greatest diameter at pathology examinations. Overall this study showed a 100% true-positive rate (2/2), 88% false-positive rate (14/16), 78% true-negative (78/94) rate, and 0% false-negative results for scintimammography. These results indicate 85% specificity, 12.5% positive predictive value, 100% negative predictive value, and 85% diagnostic accuracy for BSGI. Although the number of patients with cancer in this study was limited, the 100% sensitivity of BSGI in identifying malignancies in 2 patients with prior cancer indicates the limitations of mammography and physical examination, both of which were normal for these 2 patients. These 2 patients also had moderate breast density (BI-RADS density categories of 2 and 3), indicating the usefulness of high-resolution BSGI in all women. However, as the authors emphasize, the results of this study could be limited owing to the presence of only 2 true-positive findings.

Recent years have seen advances in the development of semiconductor detectors such as cadmium zinc telluride (CZT) for direct detection of gamma rays. Owing to its cost and relatively limited size, CZT currently seems to have best use in small, application-specific cameras such as dedicated breast or cardiac scanners. There are 2 commercially available BSGI scanners that utilize detector heads based on CZT detectors. The first of these systems was introduced by Gamma Medica under the name of LumaGEM. This scanner uses 2 opposing detector heads, each with a FOV of 20 cm × 16 cm. The individual CZT pixels are 1.6-mm wide that together with the parallel-hole collimators result in a reconstructed spatial resolution of 4.8 mm at a distance of 3 cm from the detectors. The breast is imaged with mild compression between the 2 detector heads with a 5–10 minutes scan per view. The second commercial system is the GE Discovery NM 750b Molecular Breast Imaging (MBI) sold by GE Healthcare (Fig. 4). This is also a dual-CZT detector head system with a 20-cm × 20-cm FOV and 2.5-mm wide CZT pixels. With the supplied parallel-hole collimators, the reconstructed spatial resolution is 4.4 mm at a distance of 3 cm from the detectors. Using 2 detector heads provides higher system sensitivity for the dual-detector head designs compared with single-detector head systems.

A clinical study based on 150 patients was recently performed to evaluate the benefit of the dual-detector CZT system as opposed to a single-head CZT system.[48] The aim of this study was to determine the increase in sensitivity achieved by a dual-head high-resolution BSGI system over single-head high-resolution BSGI system. Patients selected for this study had undergone sonography or mammography, had a breast lesion <2 cm in diameter and a category 4 or 5 on the BI-RADS scale, and were scheduled for a biopsy. BSGI was performed before the biopsy. The patients had a mean age of 59 years and the BI-RADS assessment of lesions was either category 4 or 5 in all patients with an almost equal

NIH-PA Author Manuscript

NIH-PA Author Manuscript

NIH-PA Author Manuscript

distribution between the 2 categories. The mammographic breast density was also almost equally split between those with >50% and <50% breast density. For BSGI, patients were injected with 20 mCi (740 MBq) of ^{99m}Tc sestamibi and each breast was imaged in the dual-head BSGI system in the CC and MLO for 10 minutes per view. Upon completion of each patient study, the images were reviewed together with images from other imaging modalities. If the BSGI image showed additional lesions that were not seen elsewhere, additional diagnostic examinations were performed to evaluate these lesions. After all 150 patients had been imaged and histopathology reports for all lesions obtained, the BSGI images were read by 3 radiologists independent of other patient information. These readings were performed blindly, first using images from only 1 detector to mimic a single-head detector followed by images from both detectors. Each BSGI image was classified with a score ranging from 1 (no focal uptake) to 5 (intense focal uptake). If abnormal uptake was observed, then the radiologist also marked the location and intensity of the abnormal uptake in the CC and MLO views. Images with lesions scoring 2 or higher were considered positive for this study. A total of 128 lesions were confirmed as cancer in 88 patients. Overall sensitivity for all tumor sizes was 80% with a single-head CZT-based BSGI system as opposed to 90% for the dual-head, CZT-based BSGI system. For tumors 6–10 mm in size, the sensitivity increased from 68%–82% with the use of 2 detector heads. For smaller lesions (≤5 mm in size), the sensitivity increases from 44%–67% with the use of 2 detector heads. Figure 5 shows an image of a patient with a 4-mm cancerous lesion that was not visible with the single-detector view but was clear with the dual-detector view. The average specificity for the dual-head system was 69%, but this value reflects the specificity in a patient population chosen to have a mammographically suspicious lesion and may not reflect what one could expect in a general screening population. This study also demonstrated the benefits of a high-resolution, dual-head BSGI system, but does not compare it directly with standard diagnostic mammography or US.

Another prospective clinical study[49] using a much larger patient population was recently completed with an aim to compare the performance of a prototype version of the dual-head GE NM Discovery 750b and mammography in screening women with mammographically dense breasts. Enrolled patients were mostly 25 years or older and were undergoing routine screening mammography, or else less than 50 years old but had not undergone mammography at the time of enrollment. Mammography was either screen based or digital with 2 views per breast. For BSGI, performed within 21 days of mammography, patients were injected with 20 mCi (740 MBq) of ^{99m}Tc sestamibi and each breast was imaged in the dual-head BSGI system in the CC and MLO for 10 minutes per view. Mammography images were independently read by trained breast radiologists in a standard manner without any knowledge of the BSGI results. A BI-RADS assessment of 0, 4, or 5 was considered to be a positive result. Images from the BSGI system were reviewed by 2 dedicated breast radiologists blinded to mammography results and assigned an abnormal tracer uptake score ranging from 1 (no abnormal uptake) to 5 (uptake highly suspicious for malignancy). Uptake scores of 3, 4, or 5 were considered to indicate a positive result. Positive cancer status in patients was defined on the basis of a positive histopathologic results from a biopsy performed within 365 days on the initial study mammography. Negative cancer status was defined as a result of: (1) negative or benign results from follow-up imaging performed within 330–365 days after the initial study mammography, (2) benign histopathologic results, or (3) medical record review or patient interview confirming no cancer diagnosis. Out of 936 patients with verified cancer status, 11 were diagnosed with positive cancer status. Three were diagnosed in mammography, 9 in BSGI, and 10 when combining both BSGI and mammography images leading to sensitivity of 27% with mammography, 82% with BSGI, and 91% with both combined. The cancers detected in BSGI images only (not visible in mammography) were invasive with size range of 0.4–5.1 cm. One cancer that was detected using mammography only involved a tumor <5 mm in size. The specificity was

NIH-PA Author Manuscript

NIH-PA Author Manuscript

NIH-PA Author Manuscript

91% for mammography only, 93% for BSGI only, and 85% for BSGI and mammography combined.

Research Systems

In parallel with the commercial BSGI systems several research laboratories have been involved in the development of research BSGI scanners. A group at the Mayo Clinic has been a primary driving force in the development of CZT-based BSGI scanners and built a single-head prototype system[50,51] before the commercial introduction of the dual-head systems from Gamma Medica and GE. The detector head used by the Mayo group is the same as the one now used in the GE NM Discovery 750b system, with the breast being imaged with mild compression and using parallel-hole collimators. A clinical study with this system[51] was performed using 100 patients with a <2-cm diameter suspicious mass detected in mammography or US (category 4 or 5 on the BI-RADS scale) and who were scheduled for a biopsy. The sensitivity of the BSGI images was 29%, 86%, and 97% for detection of <5 mm in size, 6–10 mm in size, and ≥10 mm in size lesions, respectively.

Two research groups are actively involved in development of dual modality breast-specific SPECT/CT systems that will have the advantage of providing tomographic quality single photon images with direct registration to an anatomical image. The group at the University of Virginia has developed a system that uses a single-detector head for gamma-ray imaging incorporated in a vertical, mammography-like gantry together with an x-ray source and detector.[52] The gantry provides limited rotation of the x-ray imaging system around a common axis with the compressed breast in the FOV, thereby providing a tomosynthesis image of the breast. Similarly, the gamma-ray detectors acquire data with limited rotation around the breast, and an iterative limited-angle reconstruction algorithm provides a reconstructed single photon image. Limited clinical studies have been performed with this system, as part of its design evaluation. The second system that provides full tomographic SPECT and CT images is being developed at Duke University.[53,54] This system has the patient lying prone with the breast hanging within the imaging FOV. The SPECT camera uses a single-head CZT detector that is the same as that used in the Gamma Medica LumaGEM system. Customized detector trajectories are used to collect all the projection data needed to achieve a tomographic image.

There has also been work done to reduce the dose of MIBI needed for BSGI, with the goal of reducing patient whole-body radiation exposure, an important goal if BSGI is to be considered in a screening role. These studies have shown feasibility for dose of MIBI as low as 4–8 mCi (148–296 MBq).[55]

Summary

Dedicated PEM and BSGI devices have been developed to provide higher spatial resolution and sensitivity relative to multipurpose clinical systems. BSGI systems have seen enough interest that commercially there are 3 devices currently available from different manufacturers. The improved spatial resolution of these commercial, as well as research BSGI, systems has shown some benefit of single photon imaging, primarily in the area of detection of small lesions in high-density breasts. Based on the studies completed, PEM has shown higher sensitivity or specificity or both in the detection of small lesions (1–2 cm in size) relative to mammography. The higher spatial resolution of the existing PEM systems (1.5–3 mm) has also shown that these systems can help in providing an accurate definition of the extent of disease in a breast when used together with MRI, hence being useful in surgical planning. Most of the existing dedicated PEM systems, including the only commercially available system from Naviscan, have been developed to image a compressed breast in an analogous and often in conjunction with mammography systems. New PEM

NIH-PA Author Manuscript

NIH-PA Author Manuscript

NIH-PA Author Manuscript

system designs aim to further improve the spatial resolution (around 1 mm), and in some cases also image the breast that is uncompressed and provide quantitative images. With an eye toward multimodality imaging some of these systems are considering incorporation with a full low-dose CT system, while a PEM insert compatible for use simultaneously with MRI is also being developed. The new PEM system designs hence promise to further expand the application of radionuclide imaging in the broader framework of breast cancer evaluation and treatment.

Acknowledgments

This work was supported in part by NIH grant number RO1-EB009056.

References

1. Palmedo H, Biersack HJ, Lastoria S, et al. Scintimammography with technetium-99m methoxyisobutylisonitrile: Results of a prospective European multicentre trial. Eur J Nucl Med. 1998; 25:375–385. [PubMed: 9553167]
2. Khalkhali I, Villanueva-Meyer J, Edell SL, et al. Diagnostic accuracy of Tc-99m-sestamibi breast imaging: Multicenter trial results. J Nucl Med. 2000; 41:1973–1979. [PubMed: 11138681]
3. Avril N, Dose J, Janicke F, et al. Metabolic characterization of breast tumors with positron emission tomography using F-18 fluorodeoxyglucose. J Clin Oncol. 1996; 14:1848–1857. [PubMed: 8656253]
4. Samson DJ, Flamm CR, Pisano ED, et al. Should FDG PET be used to decide whether a patient with an abnormal mammogram or breast finding at physical examination should undergo biopsy? Acad Radiol. 2002; 9:773–783. [PubMed: 12139091]
5. Jackson VP, Hendrick RE, Feig SA, et al. Imaging of the radiographically dense breast. Radiology. 1993; 188:297–301. [PubMed: 8327668]
6. Cole EB, Pisano ED, Kistner EO, et al. Diagnostic accuracy of digital mammography in patients with dense breasts who underwent problem-solving mammography: Effects of image processing and lesion type 1. Radiology. 2003; 226:153–160. [PubMed: 12511684]
7. Kolb TM, Lichy J, Newhouse JH. Comparison of the performance of screening mammography, physical examination, and breast US and evaluation of factors that influence them: An analysis of 27,825 patient evaluations. Radiology. 2002; 225:165–175. [PubMed: 12355001]
8. Baum RP, Przetak C. Evaluation of therapy response in breast and ovarian cancer patients by positron emission tomography (PET). Q J Nucl Med. 2001; 45:257–268. [PubMed: 11788818]
9. Rousseau C, Devillers A, Sagan C, et al. Monitoring of early response to neoadjuvant chemotherapy in stage II and III breast cancer by [^{18}F] fluorodeoxyglucose positron emission tomography. J Clin Oncol. 2006; 24:5366–5372. [PubMed: 17088570]
10. Khalkhali I, Mena I, Jouanne E, et al. Prone scintimammography in patients with suspicion of carcinoma of the breast. J Am Coll Surg. 1994; 178:491–497. [PubMed: 8167887]
11. Kao CH, Wang SJ, Yeh SH. Tc-99m MIBI uptake in breast carcinoma and axillary lymph node metastases. Clin Nucl Med. 1994; 19:898–900. [PubMed: 7805327]
12. Wahl RL, Cody RL, Hutchins GD, et al. Primary and metastatic breast carcinoma: Initial clinical evaluation with PET with the radio-labeled glucose analogue 2-[F-18]-fluoro-2-deoxy-D-glucose. Radiology. 1991; 179:765–770. [PubMed: 2027989]
13. Adler LP, Crowe JP, Al-Kaisi NK, et al. Evaluation of breast masses and axillary lymph nodes with [F-18] 2-deoxy-2-fluoro-D-glucose PET. Radiology. 1993; 187:743–750. [PubMed: 8497624]
14. Avril N, Rose CA, Schelling M, et al. Breast imaging with positron emission tomography and fluorine-18 fluorodeoxyglucose: Use and limitations. J Clin Oncol. 2000; 18:3495–3502. [PubMed: 11032590]
15. Tarantola G, Zito F, Gerundini P. PET instrumentation and reconstruction algorithms in whole-body applications. J Nucl Med. 2003; 44:756–769. [PubMed: 12732678]

NIH-PA Author Manuscript

NIH-PA Author Manuscript

NIH-PA Author Manuscript

16. Humm JL, Rosenfeld A, Del Guerra A. From PET detectors to PET scanners. Eur J Nucl Med. 2003; 30:1574–1597.
17. Quon A, Gambhir SS. FDG-PET and beyond: Molecular breast cancer imaging. J Clin Oncol. 2005; 23:1664–1673. [PubMed: 15755974]
18. Surti S, Kuhn A, Werner ME, et al. Performance of Philips Gemini TF PET/CT scanner with special consideration for its time-of-flight imaging capabilities. J Nucl Med. 2007; 48:471–480. [PubMed: 17332626]
19. Jakoby BW, Bercier Y, Conti M, et al. Physical and clinical performance of the mCT time-of-flight PET/CT scanner. Phys Med Biol. 2011; 56:2375–2389. [PubMed: 21427485]
20. Bettinardi V, Presotto L, Rapisarda E, et al. Physical performance of the new hybrid PET/CT discovery-690. Med Phys. 2011; 38(10):5394–5411. [PubMed: 21992359]
21. Thompson CJ, Murthy K, Weinberg IN, et al. Feasibility study for positron emission mammography. Med Phys. 1994; 21:529–538. [PubMed: 8058019]
22. Robar JL, Thompson CJ, Murthy K, et al. Construction and calibration of detectors for high-resolution metabolic breast cancer imaging. Nucl Instrum Meth A. 1997; 392:402–406.
23. Weinberg I, Majewski S, Weisenberger A, et al. Preliminary results for positron emission mammography: Real-time functional breast imaging in a conventional mammography gantry. Eur J Nucl Med Mol Imag. 1996; 23:804–806.
24. Turkington, TG.; Majewski, S.; Weisenberger, AG., et al. A large field of view positron emission mammography imager. Presented at 2003 IEEE Nuclear Science Symposium and Medical Imaging Conference; Portland, OR. Oct 19–25, 2003;
25. Berg WA, Weinberg IN, Narayanan D, et al. High-resolution fluorodeoxyglucose positron emission tomography with compression ("positron emission mammography") is highly accurate in depicting primary breast cancer. Breast J. 2006; 12:309–323. [PubMed: 16848840]
26. Berg WA, Madsen KS, Schilling K, et al. Breast cancer: Comparative effectiveness of positron emission mammography and MR imaging in presurgical planning for the ipsilateral breast. Radiology. 2011; 258:59–72. [PubMed: 21076089]
27. Abreu MC, Aguiar JD, Almeida FG, et al. Design and evaluation of the clear-PEM scanner for positron emission mammography. IEEE Trans Nucl Sci. 2006; 53:71–77.
28. Wu Y, Bowen SL, Yang K, et al. PET characteristics of a dedicated breast PET/CT scanner prototype. Phys Med Biol. 2009; 54:4273–4287. [PubMed: 19531852]
29. Bowen SL, Wu Y, Chaudhari AJ, et al. Initial characterization of a dedicated breast PET/CT scanner during human imaging. J Nucl Med. 2009; 50:1401–1408. [PubMed: 19690029]
30. Raylman RR, Abraham J, Hazard H, et al. Initial clinical test of a breast PET scanner. J Med Imaging Radiat Oncol. 2011; 55:58–64. [PubMed: 21382190]
31. Wang GC, Huber JS, Moses WW, et al. Characterization of the LBNL PEM camera. IEEE Trans Nucl Sci. 2006; 53:1129–1135.
32. Moliner L, González AJ, Soriano A, et al. Design and evaluation of the MAMMI dedicated breast PET. Med Phys. 2012; 39:5393–5404. [PubMed: 22957607]
33. Freifelder, R.; Cardi, C.; Grigoras, I., et al. First results of a dedicated breast PET imager (B-PET) using NaI(Tl) curve-plate detectors. Presented at 2001 IEEE Nuclear Science Symposium and Medical Imaging Conference; San Diego, CA. Nov 04–10, 2001;
34. Srinivas, SM.; Freifelder, R.; Saffer, JR., et al. A dedicated breast positron emission tomography (B-PET) scanner: Characterization and pilot patient study. Presented at 2006 IEEE Nuclear Science Symposium and Medical Imaging Conference; San Diego, CA. Oct 29–Nov 05, 2006;
35. Lima M, Nakamoto Y, Kanao S, et al. Clinical performance of 2 dedicated PET scanners for breast imaging: Initial evaluation. J Nucl Med. 2012; 53:1534–1542. [PubMed: 22933819]
36. Zhang J, Olcott PD, Chinn G, et al. Study of the performance of a novel 1 mm resolution dual-panel PET camera design dedicated to breast cancer imaging using Monte Carlo simulation. Med Phys. 2007; 34:689–702. [PubMed: 17388187]
37. Surti S, Karp JS. Design considerations for a limited angle, dedicated breast, TOF PET scanner. Phys Med Biol. 2008; 53:2911–2921. [PubMed: 18460745]

NIH-PA Author Manuscript

NIH-PA Author Manuscript

NIH-PA Author Manuscript

38. Krishnamoorthy, S.; Wiener, RI.; Kaul, M., et al. Development of a high-resolution and depth-of-interaction capable detector for time-of-flight PET. Presented at 2011 IEEE Nuclear Science Symposium and Medical Imaging Conference; Valencia, Spain. Oct 23–29, 2011;
39. Godinez F, Chaudhari AJ, Yang Y, et al. Characterization of a high-resolution hybrid DOI detector for a dedicated breast PET/CT scanner. Phys Med Biol. 2012; 57:3435–3449. [PubMed: 22581109]
40. Ravindranath B, Huang P-J, Junnarkar S, et al. Quantitative clinical evaluation of a simultaneous PET/MRI breast imaging system. J Nucl Med. 2012; 53:1217. [abstract].
41. Ravindranath B, Junnarkar S, Purschke M, et al. Results from a simultaneous PET-MRI breast scanner. J Nucl Med. 2011; 52:432. [abstract].
42. Tai YC, Wu H, Pal D, et al. Virtual-pinhole PET. J Nucl Med. 2008; 49:471–479. [PubMed: 18287272]
43. Ravindranath B, Wen J, Mathews A, et al. A flat panel virtual-pinhole PET insert for axillary and internal mammary lymph node imaging in breast cancer patients. J Nucl Med. 2012; 53:432. [abstract].
44. Taillefer R. The role of ^{99m}Tc-sestamibi and other conventional radio-pharmaceuticals in breast cancer diagnosis. Semin Nucl Med. 1999; 29:16–40. [PubMed: 9990681]
45. Waxman AD. The role of ^{99m}Tc methoxyisobutylisonitrile in imaging breast cancer. Semin Nucl Med. 1997; 27:40–54. [PubMed: 9122723]
46. Majewski S, Kieper D, Curran E, et al. Optimization of dedicated scintimammography procedure using detector prototypes and compressible phantoms. IEEE Trans Nucl Sci. 2001; 48:822–829.
47. Brem RF, Rapelyea JA, Zisman G, et al. Occult breast cancer: Scintimammography with high-resolution breast-specific gamma camera in women at high risk for breast cancer. Radiology. 2005; 237:274–280. [PubMed: 16126919]
48. Hruska CB, Phillips SW, Whaley DH, et al. Molecular breast imaging: Use of a dual-head dedicated gamma camera to detect small breast tumors. AJR Am J Roentgenol. 2008; 191:1805–1815. [PubMed: 19020253]
49. Rhodes DJ, Hruska CB, Phillips SW, et al. Dedicated dual-head gamma imaging for breast cancer screening in women with mammographically dense breasts. Radiology. 2011; 258:106–118. [PubMed: 21045179]
50. Mueller B, O'Connor MK, Blevis I, et al. Evaluation of a small cadmium zinc telluride detector for scintimammography. J Nucl Med. 2003; 44:602–609. [PubMed: 12679406]
51. O'Connor MK, Phillips SW, Hruska CB, et al. Molecular breast imaging: Advantages and limitations of a scintimammographic technique in patients with small breast tumors. Breast J. 2007; 13:3–11. [PubMed: 17214787]
52. Williams MB, Judy PG, Gunn S, et al. Dual-modality breast tomosynthesis. Radiology. 2010; 255:191–198. [PubMed: 20308457]
53. Tornai MP, Bowsher JE, Jaszczak RJ, et al. Mammotomography with pinhole incomplete circular orbit SPECT. J Nucl Med. 2003; 44:583–593. [PubMed: 12679403]
54. Cutler SJ, Perez KL, Barnhart HX, et al. Observer detection limits for a dedicated SPECT breast imaging system. Phys Med Biol. 2010; 55:1903–1916. [PubMed: 20224159]
55. Hruska CB, Weinmann AL, Skjerseth CMT, et al. Proof of concept for low-dose molecular breast imaging with a dual-head CZT gamma camera. Part II. Evaluation in patients. Med Phys. 2012; 39:3476–3483. [PubMed: 22755727]

NIH-PA Author Manuscript

NIH-PA Author Manuscript

NIH-PA Author Manuscript

Figure 1.
A picture of the Naviscan Flex Solo II PEM scanner. Image reproduced from Naviscan PET Systems, Inc. product brochure. (Published with permission from NaviScan.) (Color version of the figure is available online.)

NIH-PA Author Manuscript

NIH-PA Author Manuscript

NIH-PA Author Manuscript

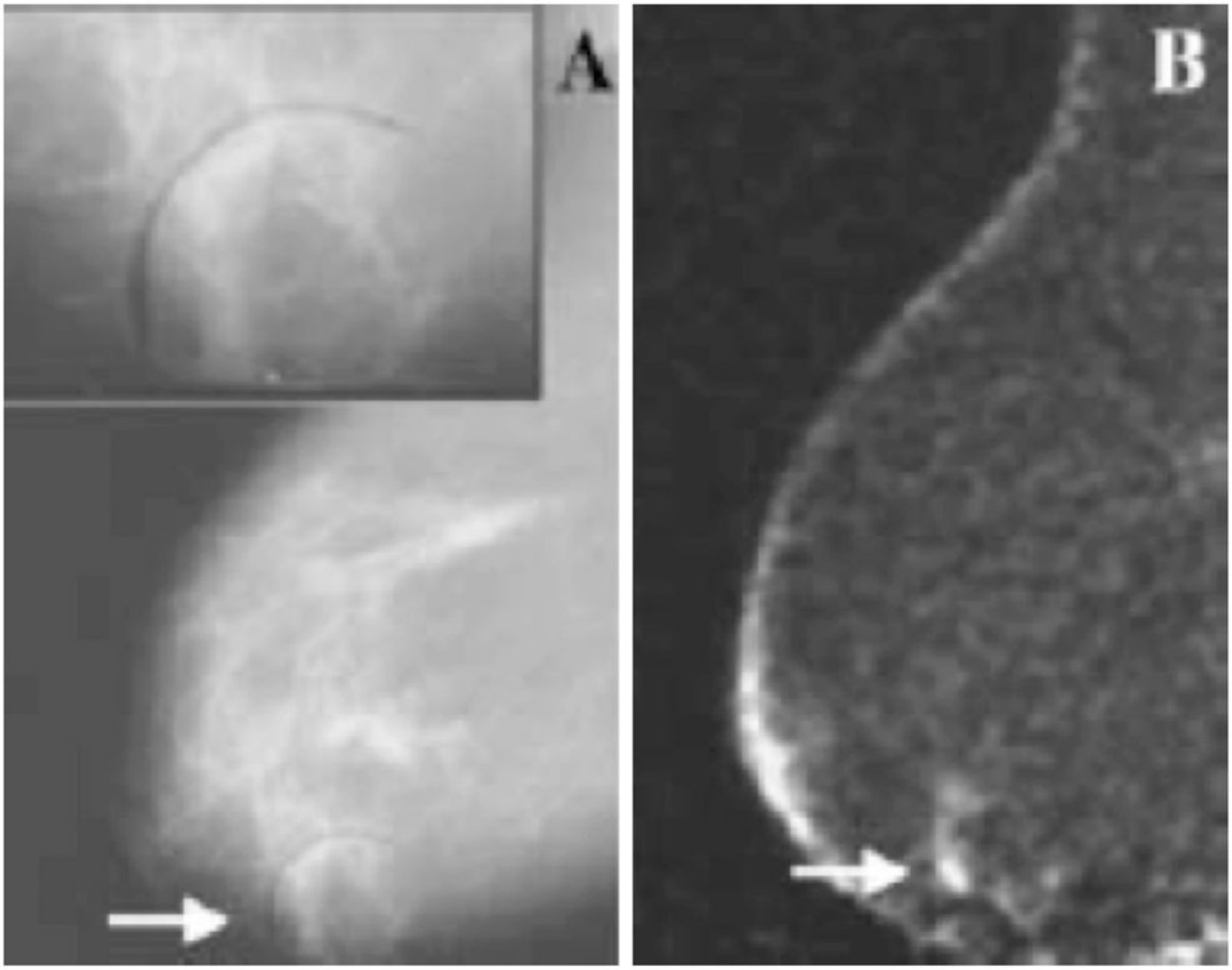

Figure 2.
(A) MLO mammogram of a patient with DCIS with microcalcifications marked by the arrow. (B) PEM image acquired on the Naviscan Flex Solo II PEM scanner showing intense focal uptake at the site of calcifications shown in the mammogram. Intermediate grade DCIS was confirmed with needle biopsy. Reprinted with permission from Berg et al.[25]

NIH-PA Author Manuscript

NIH-PA Author Manuscript

NIH-PA Author Manuscript

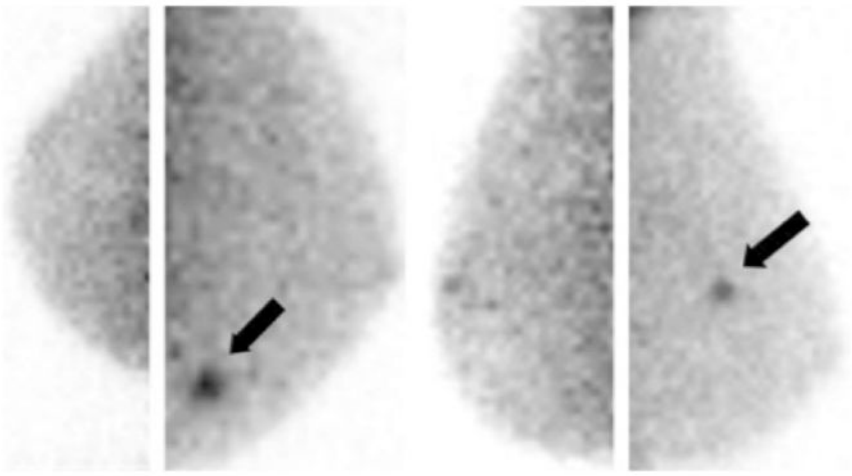

Figure 3.
Abnormal, focused radiotracer uptake seen in a scintimammogram for a patient acquired on a Dilon 6800 system. Images from left to right show left CC, right CC, left MLO, and right MLO views. Pathology demonstrated 9 mm infiltrating ductal carcinoma. Reprinted with permission from Brem et al.[47]

NIH-PA Author Manuscript

NIH-PA Author Manuscript

NIH-PA Author Manuscript

Figure 4.
A picture of the GE Discovery NM 750b dual head CZT-based MBI. (Image provided by GE Healthcare.) (Color version of the figure is available online.)

NIH-PA Author Manuscript

NIH-PA Author Manuscript

NIH-PA Author Manuscript

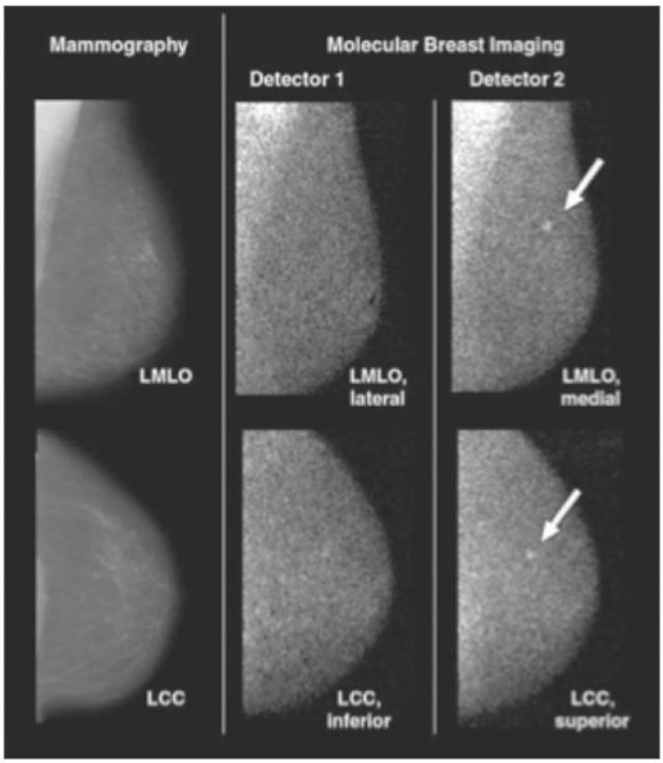

Figure 5.
An 82-year-old patient with 4-mm invasive lobular carcinoma as marked by the arrows. Molecular breast imaging findings were negative when only images from detector 1 were available. However, together with detector 2, cancer was identified with a high focal uptake. Reprinted with permission from Hruska et al.[48] (Color version of the figure is available online.)

NIH-PA Author Manuscript

NIH-PA Author Manuscript

NIH-PA Author Manuscript

Table 1

Summary of Results for Additional Cancer Found in Patients Imaged as Part of a Large Study Evaluating the use of PEM in Surgical Planning for Breast Cancer Patients[26]

		Sensitivity (%)	Specificity (%)	Accuracy (%)
Detection of breasts with additional lesions	Mammography	27	97.4	82.5
	PEM	51	91.2	82.7
	MRI	60	86.3	80.7
	PEM + MRI	74	83.3	81.4
	PEM + MRI + Mammography	83	82.4	82.5
	PEM + Mammography	65	89.9	84.5
	MRI + Mammography	72	84.6	82.0
Detection of additional malignant lesions	Mammography	21	94.2	66.2
	PEM	41	79.9	64.9
	MRI	53	65.6	60.7
	PEM + MRI	66	61.4	63.0
	PEM + MRI + Mammography	73	58.7	64.3
	PEM + Mammography	52	75.7	66.6
	MRI + Mammography	63	61.4	62.0